


## RESEARCH ARTICLE

# Electrofermentation increases concentration of poly $\gamma$ -glutamic acid in *Bacillus subtilis* biofilms

Alina Adilkhanova<sup>1</sup> | Anar Ormantayeva<sup>1</sup> | Aisholpan Kaziullayeva<sup>1</sup> |  
Kayode Olaifa<sup>1</sup> | Neda Eghtesadi<sup>1</sup> | Azza H. Abbas<sup>2</sup> | Cinzia Calvio<sup>3</sup> |  
Tri T. Pham<sup>4</sup> | Obinna M. Ajunwa<sup>1,5</sup> | Enrico Marsili<sup>6</sup> 

<sup>1</sup>Biofilm Laboratory, Department of Chemical and Materials Engineering, School of Engineering and Digital Sciences, Nazarbayev University, Astana, Kazakhstan

<sup>2</sup>Department of Petroleum Engineering, School of Mining and Geosciences, Nazarbayev University, Astana, Kazakhstan

<sup>3</sup>Nottingham Ningbo China Beacons of Excellence Research and Innovation Institute, Ningbo, China

<sup>4</sup>Department of Biology and Biotechnology, Università degli Studi di Pavia, Pavia, Italy

<sup>5</sup>Department of Biology, School of Sciences and Humanities, Nazarbayev University, Astana, Kazakhstan

<sup>6</sup>Department of Biology, Faculty of Natural Sciences, Interdisciplinary Nanoscience Center, Aarhus University, Aarhus, Denmark

## Correspondence

Enrico Marsili, Nottingham Ningbo China Beacons of Excellence Research and Innovation Institute, No. 211, Xingguang Road, Yinzhou District, Ningbo, China.  
Email: [enrico.marsili1@gmail.com](mailto:enrico.marsili1@gmail.com)

## Funding information

Collaborative Research Program, Nazarbayev University, Grant/Award Number: 021220CRP0522; Nottingham Ningbo China Beacons of Excellence Research and Innovation Institute, Grant/Award Number: I01220800007

## Abstract

Fluctuations in redox conditions in bioprocesses can alter the end-products, reduce their concentration, and lengthen the process time. Electrofermentation enables rapid metabolic modulation of biosynthesis and allows control of redox imbalances in biofilm-based fermentation processes. In this study, electrofermentation is used to boost the production of the bacterial biopolymer poly- $\gamma$ -glutamic acid ( $\gamma$ -PGA) from *Bacillus subtilis* ATCC 6051. When compared to control experiments ( $3.3 \pm 0.99 \text{ g L}^{-1}$ ), the application of an electrode potential  $E = 0.4 \text{ V}$  versus Ag/AgCl results in a more than two-fold increase in the production of  $\gamma$ -PGA ( $9.13 \pm 1.4 \text{ g L}^{-1}$ ). Using an engineered *B. subtilis* strain, in which  $\gamma$ -PGA production is driven by isopropyl  $\beta$ -D-1-thiogalactopyranoside, electrofermentation improves polymer concentrations from  $15.4 \pm 1.5$  to  $23.1 \pm 1.6$  versus  $\text{g L}^{-1}$ . These results confirm that electrofermentation conditions can be adopted to increase the concentration of  $\gamma$ -PGA and perhaps other extracellular biopolymers in industrial strains.

## INTRODUCTION

Biopolymers are important in applications in wastewater treatment (Xia et al., 2020), in the food industry as packaging agents or emulsifiers (Westlake et al., 2023), and in tissue engineering as well as targeted drug development (Biswas et al., 2022). Recent advances in microbial fermentation have offered more sustainable approaches for the production of biopolymers (Wang, Hwang, et al., 2020).

Poly- $\gamma$ -glutamic acid ( $\gamma$ -PGA) is a biodegradable anionic biopolymer synthesized from L-glutamic acid, D-glutamic acid, or both, by forming  $\gamma$ -amide bonds (Qiu et al., 2019). Due to its solubility in water, biodegradability, its metal binding properties, viscous texture, zero toxicity, and devoid of immunogenic compounds,  $\gamma$ -PGA is used as a biomaterial to develop drug carriers (Wang et al., 2021) or construct scaffolds for tissue engineering (Liu et al., 2021; Zhu et al., 2021). Commercial  $\gamma$ -PGA is produced through the microbial fermentation

This is an open access article under the terms of the [Creative Commons Attribution-NonCommercial](https://creativecommons.org/licenses/by-nc/4.0/) License, which permits use, distribution and reproduction in any medium, provided the original work is properly cited and is not used for commercial purposes.

© 2024 The Authors. *Microbial Biotechnology* published by John Wiley & Sons Ltd.

of biomass by *Bacillus* species (Luo et al., 2016; Nair et al., 2021). Although chemical synthesis may produce  $\gamma$ -PGA with controllable chain length (Sanda et al., 2001), microbial fermentation is preferred because of the higher molecular weight of  $\gamma$ -PGA and high production rate.

The microorganisms used for the fermentation of  $\gamma$ -PGA are mostly *Bacillus* species such as *B. licheniformis*, *B. subtilis*, *B. amyloliquefaciens*, which secrete  $\gamma$ -PGA in a strain-dependent manner. While increasing the glutamate concentration in the media can increase  $\gamma$ -PGA synthesis, this procedure also raises the overall cost of  $\gamma$ -PGA bioproduction (Luo et al., 2016). Therefore, ongoing research aims to enhance the production of  $\gamma$ -PGA through the isolation of new strains, medium optimization (Wang, Kim, et al., 2020), genetic engineering of metabolic pathways (Gao et al., 2019), and induction of environmental shocks to upregulate the  $\gamma$ -PGA synthetase operon (Song et al., 2020; Tang et al., 2016). Previously, genetically modified organisms have been employed to overcome the constraints of the metabolic flux between substrates and products. For instance, deleting the *pgdS* and *ggt* PGA hydrolase genes of *B. subtilis* resulted in lower levels of  $\gamma$ -PGA hydrolysis and a 50% increase in  $\gamma$ -PGA concentration (Scoffone et al., 2013). However, there is still an inherent limitation in most fermentation systems, which may be linked to the ineffective control of intracellular and extracellular redox activities and reactions (Li et al., 2018). For example, in aerobic fermentation, energy can be directed into formation of undesired biomass and carbon dioxide instead of the target product (Weusthuis et al., 2011). In anaerobic fermentation, microorganisms can synthesize reduced products, which can also be detrimental to the yield of the desired product (Förster & Gescher, 2014).

It is possible to avoid limitations of conventional fermentation (F) and redirect carbon metabolism towards synthesizing desired end-products by controlling redox metabolic reactions and energy efficiency via electrofermentation (EF) (Vassilev et al., 2021). In EF, electrodes act as electron sinks or sources in a controlled fashion (Choi et al., 2014). This causes bioelectrochemical reactions that induce the generation of a range of metabolites from bacteria such as ethanol (Flynn et al., 2010) and acetate (Sturm-Richter et al., 2015), among others. As microbial cells interact with the electrodes, the cellular redox imbalance is regulated by setting the electrodes at specific potentials to alter redox activities during fermentation (Moscoviz et al., 2016; Vassilev et al., 2021). EF is particularly effective to enhance biosynthetic process in electroactive microorganisms, i.e., those organisms capable of extracellular electron transfer (EET) to and from polarized electrodes through surface-bound protein structures or via soluble or membrane-bound redox mediators. Since very few microorganisms produce extracellular

redox mediators in sufficient concentration, redox mediators are exogenously added, which increases the environmental burden and cost of EF processes (Logan et al., 2019). While bioprocess industry workhorses like *Saccharomyces cerevisiae*, *E. coli*, and *B. subtilis* have been recently reclassified as weak electroactive microorganisms, their constitutive electroactivity without the addition of redox mediators can be too low for practical EF applications (Doyle & Marsili, 2018).

A typical EF reactor comprises a high surface working electrode (WE), a counter electrode (CE) and a reference electrode (RE). Metabolically, the potential applied through the WE can modulate intracellular  $\text{NAD}^+/\text{NADH}$  ratios and extracellular redox potentials, which, in turn, could influence the synthesis of specific metabolites. To be economically feasible, EF should be carried out in the presence of biofilms. A few products have been produced using the EF technique. Choi et al., 2014 utilized EF in the conversion of glucose to butanol using *Clostridium pasteurianum*. Applied potentials have also been utilized in EF production of ethanol from glycerol by *Shewanella oneidensis* (Flynn et al., 2010). EF has also been applied in the production of intracellular polymers like polyhydroxybutyrate (PHB) from *Ralstonia* species (Miyahara et al., 2020). These works show the potential value of EF in production of both intracellular and extracellular metabolites if properly optimized. Biofilms as interfacial microbial communities have microbial cells encased in self-produced extracellular polymeric substances (EPS) (Flemming et al., 2016). In biofilms, the EET process occurs over a short distance, thus increasing the EET rate and conversion rate of substrate(s) into product(s) (Vassilev et al., 2021). As EET is an interfacial process, biofilms can be induced as the framework for EF production. Such biofilms should be kept thin to maximize the surface/volume ratio, thus the conversion rate (Yu et al., 2017).

EPS is a term loosely used to describe all extracellularly produced polymeric materials bound to the cell in the biofilm (Flemming et al., 2016). In bioelectrochemical studies, EPS production has proved pivotal, as many electroactive bacteria can produce EPS as one of the identified mechanisms for electroactivity (Vassilev et al., 2021).

The production of  $\gamma$ -PGA within the EPS matrix of weak electroactive microorganisms through EF is theoretically possible but has not been reported, to the best of our knowledge. Here, we report for the first time the application of EF to produce PGA in *Bacillus* species. The novelty of this work lies in the targeted production of PGA within the EPS matrix by careful control of electroactivity in *Bacillus subtilis*. We specifically used the wild-type (WT) strain *B. subtilis* ATCC 6051 and a genetically modified (GM) strain, PB5760, in which  $\gamma$ -PGA production can be induced by isopropyl  $\beta$ -D-1-thiogalactopyranoside (IPTG), to produce  $\gamma$ -PGA under

F and EF conditions. The effect of the electrode potential on  $\gamma$ -PGA concentration within EPS was assessed in comparison with production under open circuit potentials (OCP), which is equivalent to F. The current and charge output during the EF process and electrochemical impedance spectroscopy (EIS) measurements of EPS extracts after the  $\gamma$ -PGA production give further insight into the EF process. The  $\gamma$ -PGA concentration correlates positively with the electrode potential and the charge output measured.

## EXPERIMENTAL PROCEDURES

### Microorganism and culture conditions

*B. subtilis* ATCC 6051 (WT) was obtained by the *Bacillus* Genetic Stock Center (<https://bgsc.org/>), sub-cultured on sterile nutrient broth as seed medium and maintained on nutrient agar slants for storage at 4°C. The genetically modified strain *B. subtilis* PB5760 was sub-cultured according to the same protocol. This is a derivative of the transformable wild strain DK1042 (Konkol et al., 2013), in which the pMATywsC plasmid (Ermoli et al., 2021) was inserted by single crossing-over. In the pMATywsC, the endogenous *pgs* operon is posed under the control of IPTG while the endogenous *pgs* promoter controls a translational fusion of part of the *pgsB* gene to a superfolder GFP. In the presence of 0.3 mM IPTG, PB5760 overproduces  $\gamma$ -PGA; conversely, no polymer production occurs without IPTG.

The fermentation medium for  $\gamma$ -PGA production with *B. subtilis* ATCC 6051 comprised (per L): 0.25 M glucose, 0.3 M L-glutamic acid, 0.1 M  $\text{NH}_4\text{Cl}$ , 3 mM  $\text{K}_2\text{HPO}_4$ , 2 mM  $\text{MgSO}_4 \cdot 7\text{H}_2\text{O}$ , 0.15 mM  $\text{FeSO}_4 \cdot 6\text{H}_2\text{O}$ , 1 mM  $\text{CaCl}_2 \cdot 2\text{H}_2\text{O}$ , 0.72 mM  $\text{MnCl}_2 \cdot \text{H}_2\text{O}$ , and 9 mM NaCl was prepared with deionized water before sterilization at 121°C and 104 kPa for 20 min (Wang, Kim, et al., 2020). IPTG was sterile-filtered and added (0.3 mM) to the fermentation medium for  $\gamma$ -PGA production in the genetically engineered strain *B. subtilis* PB5760. Control experiments without IPTG were also conducted. For inoculation, a loopful of *B. subtilis* culture from nutrient agar slants was transferred into 30 mL nutrient broth in 50 mL tubes and incubated for 24 h at 37°C with 200 rpm shaking. The fermentation medium (80 mL) in 250 mL flasks was inoculated with actively growing seed culture, adjusted to an optical density of  $5.0 \pm 0.1$  ( $\text{OD}_{600}$ ) and then set for 48 h of incubation at 35°C with 200 rpm shaking. Following cold ethanol extraction (see Section 2.3) and after dissolution in deionized water, the concentration of  $\gamma$ -PGA in flasks was determined by UV/Vis spectrophotometer at 216 nm against a PGA standard (Zeng et al., 2012).

Glucose, fructose, maltose, and glycerol were tested separately as carbon source at 0.25 M concentration. Ammonium sulfate ( $(\text{NH}_4)_2\text{SO}_4$ ), sodium nitrate

( $\text{NaNO}_3$ ), ammonium chloride ( $\text{NH}_4\text{Cl}$ ), all at 0.1 M concentration, and 5.2 g L<sup>-1</sup> each of peptone, casein, yeast extract, were tested as nitrogen source. The effect of pH (5.4–9.4) and temperature (25–55°C) was also tested. *B. subtilis* ATCC 6051 was used for all optimization experiments. The EF and F experiments on both strains (*B. subtilis* ATCC 6051 and *B. subtilis* PB5760) were carried out under optimal conditions, having the best performing carbon sources, nitrogen sources, temperature, and pH. Control experiments were carried out using the two strains with and without IPTG. Results are shown as the mean value for three independent biological replicates  $\pm$  standard error (SE).

### EF experiments

The redox mediator, 2-hydroxy-1,4-naphthoquinone (HNQ) (Sigma Aldrich), was added at 50  $\mu\text{M}$  in all the experiments. The electrochemical cells were fitted with 9.6 cm<sup>2</sup> carbon felt WE, platinum CE and Ag/AgCl RE. Electrodes and chambers were sterilized with ethanol and UV-b exposure for 30 min. All electrochemical experiments were performed in 80 mL volume at 35°C without agitation with a multichannel VSP potentiostat (Bio-logic) and 5.0  $\text{OD}_{600}$  inoculum size. Chronoamperometry (CA) was performed at WE potentials ranging from -400 to 600 mV versus Ag/AgCl for 48 h. The specific oxidation current ( $\mu\text{A cm}^{-2}$ ) and charge output ( $\text{mC cm}^{-2}$ ) were recorded for three independent biological replicates. The  $\gamma$ -PGA concentration in the EPS was determined spectrophotometrically and confirmed with Fourier Transform Infrared (FT-IR) and Proton Nuclear Magnetic Resonance (<sup>1</sup>H)-NMR.

### Extraction and quantification of $\gamma$ -PGA enriched EPS in biofilm

The EPS was extracted and analysed (Li et al., 2016; Yu et al., 2016). In short, the biofilm was sonicated for 3 min at 20 kHz and then centrifuged at 4800 rpm for 5 min. Formaldehyde (1% w/w) was added to the supernatant before incubating for 45 min at 4°C. Afterwards, three volumes of ethanol (4°C) were added to the mixture, which was then centrifuged at 4800 rpm at 4°C for 30 min to obtain a pellet. The procedure was repeated twice, then the pellet was dried under vacuum and re-suspended in deionized water, and the  $\gamma$ -PGA concentration was determined by UV/Vis spectrophotometer at 216 nm against a PGA standard (Zeng et al., 2012).

FT-IR spectra of the  $\gamma$ -PGA enriched EPS were collected using a Nicolet iS10 FT-IR, in the region 4000–400 cm<sup>-1</sup>. The samples were also characterized by (<sup>1</sup>H)-NMR, using a JMN-ECA 500 spectrometer. The  $\gamma$ -PGA-enriched EPS (5 mg) was dissolved in 0.6 mL

deuterium oxide (D<sub>2</sub>O). The (<sup>1</sup>H)-NMR Spectra were obtained from eight scans for each sample.

## Electrochemical characterization of $\gamma$ -PGA enriched EPS

EIS experiments were performed on the extracted EPS samples using graphite screen-printed electrodes (SPE) (Metrohm) at 25 ± 1°C, with a 0.126 cm<sup>2</sup> WE. The impedance spectra were obtained in a frequency range from 100 kHz to 100 mHz with sinusoidal potential of 10 mV amplitude. For each measure, 1 mg of dried extract was dissolved in 80  $\mu$ L of sterile deionized water and then drop-casted onto the SPE. All measurements were performed in 0.1 M KCl electrolyte mixed with the redox mediator 0.1 mM, K<sub>4</sub>[Fe(CN)<sub>6</sub>]·3H<sub>2</sub>O. The equivalent electrical circuit R1 + (Q2/R2) was used (Scheme S1). The average value of the effective capacitance (C<sub>eff</sub>) at interface was calculated using the Hsu-Mansfeld equation (see Equation 1, supplementary information).

## Microscope analyses

After EF experiments, the WE with *B. subtilis* biofilms containing the  $\gamma$ -PGA-enriched EPS were imaged using Scanning Electron Microscopy (SEM), using standard protocol (see supplementary information for details), with a Crossbeam 540 (Carl Zeiss).

## RESULTS AND DISCUSSION

### Optimization of physiological conditions

The effect of temperature, pH, carbon source, and nitrogen source on  $\gamma$ -PGA concentrations in *B. subtilis* ATCC 6051 under F mode was evaluated. At 37°C, the maximum  $\gamma$ -PGA concentration (0.90 ± 0.08 g L<sup>-1</sup>) was obtained at pH 7.4 (Figure 1A). This is likely related to the influence of pH on cell membrane charge. Richard and Margaritis had previously shown that *B. subtilis* IFO 3335 produces the maximum amount of  $\gamma$ -PGA at pH 7.0, which also supports the formation of highest biomass (Richard & Margaritis, 2003).

The maximum  $\gamma$ -PGA production (1.15 ± 0.07 g L<sup>-1</sup>) was obtained at 35°C (Figure 1B). *B. subtilis* is a mesophilic species; thus, many of its inductive and constitutive enzymes perform optimally at temperature ranges between 30 and 40°C (Wang, Kim, et al., 2020). Odeniyi and Avoseh (2018) reported the highest  $\gamma$ -PGA production in *B. toyonensis* As8 at 25°C. However,  $\gamma$ -PGA production was also reported in thermophilic *Bacillus* sp. strains, where  $\gamma$ -PGA concentration increased at 40–45°C (Wang, Kim, et al., 2020). Metabolic fluxes

leading to  $\gamma$ -PGA production can be controlled by regulating the growth temperature (Zeng et al., 2014). Glucose was the optimal carbon source for  $\gamma$ -PGA, with a production of 0.7 ± 0.05 g L<sup>-1</sup> (Figure 1C). In  $\gamma$ -PGA synthesis, carbon sources enter the TCA cycle to form  $\alpha$ -ketoglutaric acid, which is converted into glutamic acid by the enzyme glutamate dehydrogenase, leading to the formation of  $\gamma$ -PGA via polymerization activated by  $\gamma$ -PGA synthase (Mohanraj et al., 2019).

Glucose has been reported to be the best carbon nutrient followed by fructose and starch in comparison with lactose and maltose (Ju et al., 2014; Odeniyi & Avoseh, 2018; Wang et al., 2020b). Nitrogen sources are important for the synthesis of peptides and amino acids, which are the building blocks of enzymes that participate in all cellular reactions (Arnold et al., 2015). On its own, glutamic acid in the medium is a nitrogen source for *B. subtilis* metabolism. In  $\gamma$ -PGA production, however, glutamic acid also augments cellular  $\gamma$ -PGA biosynthesis (Luo et al., 2016). A complementary nitrogen source would therefore be required to balance the synthesis of additional amino acids and favouring the production of more enzymes involved in the  $\gamma$ -PGA biosynthesis. In this work, the maximum  $\gamma$ -PGA concentration, 6.39 ± 0.94 g L<sup>-1</sup>, was achieved with the nitrogen source supplementation of (NH<sub>4</sub>)<sub>2</sub>SO<sub>4</sub> (Figure 1D).

Previous studies suggested that inorganic nitrogen sources could function in the improvement in  $\gamma$ -PGA production (Ju et al., 2014; Wang, Kim, et al., 2020). However, the low performance of NH<sub>4</sub>Cl could be attributed to the influence of the anions of the ammonium compounds, i.e., Cl<sup>-</sup>, as those could affect permeability and membrane absorption. Even though complex nitrogen sources could induce higher productivity, we observed that (NH<sub>4</sub>)<sub>2</sub>SO<sub>4</sub> had a comparatively better performance in comparison with the complex nitrogen sources tested. The mechanisms of (NH<sub>4</sub>)<sub>2</sub>SO<sub>4</sub> inducements for  $\gamma$ -PGA production in biofilms as observed here have not been fully elucidated. We suggest that the ease of conversion of (NH<sub>4</sub>)<sub>2</sub>SO<sub>4</sub> into absorbable ammonium, without releasing noxious anions, could make it a functional nitrogen source in  $\gamma$ -PGA production. Ammonia is extracted from (NH<sub>4</sub>)<sub>2</sub>SO<sub>4</sub> in a one-step process, and the readily diffusible ammonium can be imported into the cytosol and converted to glutamine, by glutamine synthetase. Converting complex nitrogen sources to ammonium/glutamine might also require additional enzymatic reactions, which consume energy, thus lowering the overall  $\gamma$ -PGA concentration (Bajaj et al., 2009). With glutamic acid already present in the fermentation medium, the cell could direct most of its enzymatic machinery towards biofilm  $\gamma$ -PGA production with ease, thereby making complex nitrogen sources less desirable than (NH<sub>4</sub>)<sub>2</sub>SO<sub>4</sub> in this case. We however acknowledge that the observed effect with (NH<sub>4</sub>)<sub>2</sub>SO<sub>4</sub> inducement of  $\gamma$ -PGA production in biofilms may be strain-dependent, as well as depending on the

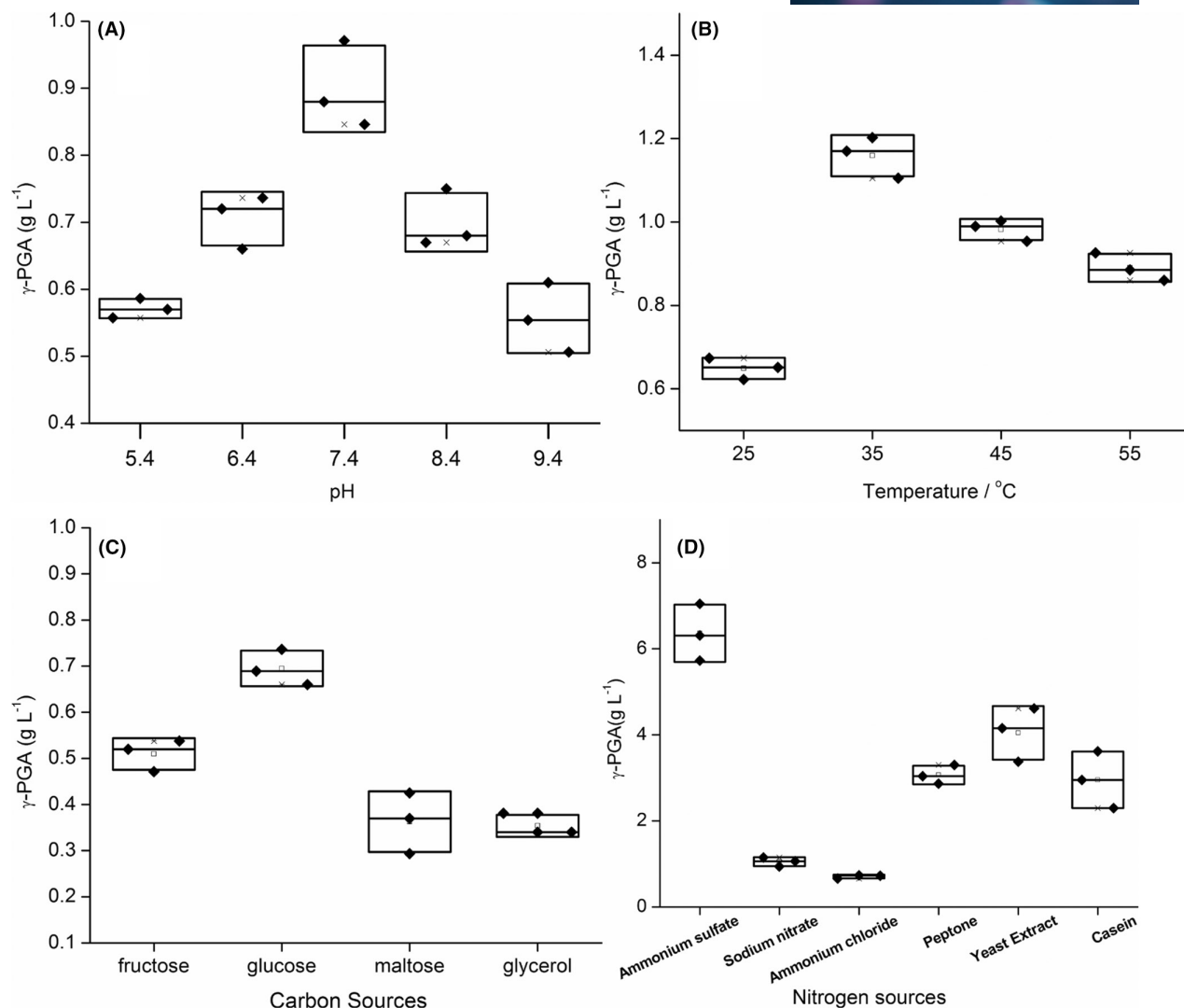


**FIGURE 1** Influence of (A) pH, (B) temperature, (C) carbon sources, (D) nitrogen source, on  $\gamma$ -PGA production (g L<sup>-1</sup>) by *B. subtilis* ATCC 6051 after 48 h under F conditions. Experiments (A) were performed at 37°C with glucose as carbon source and NH<sub>4</sub>Cl as nitrogen source. Experiments (B) were performed at pH 6.4, glucose as carbon source, and NH<sub>4</sub>Cl as nitrogen source. Experiments (C) were performed at pH 6.4, 37°C, and NH<sub>4</sub>Cl as nitrogen source. Experiments (D) were performed at pH 6.4, 37°C, and glucose as carbon source.

dynamics of biofilm growths, thereby making it important for further studies.

### Characterization of $\gamma$ -PGA enriched EPS

The optimal medium composition for EF experiments included 0.25 M glucose, 0.3 M L-glutamic acid, 0.1 M (NH<sub>4</sub>)<sub>2</sub>SO<sub>4</sub>, 3 mM K<sub>2</sub>HPO<sub>4</sub>, 2 mM MgSO<sub>4</sub>·7H<sub>2</sub>O, 0.15 mM FeSO<sub>4</sub>·6H<sub>2</sub>O, 1 mM CaCl<sub>2</sub>·2H<sub>2</sub>O, 0.72 mM MnCl<sub>2</sub>·H<sub>2</sub>O and 9 mM NaCl. The optimum temperature and optimum initial pH were set at 35°C and 7.4, respectively. The incubation time was set at 48 h. Due to the difficulty of maintaining the electrode connections with the potentiostat under stirring conditions, the EF experiments were carried out under static conditions.

Except for 600 mV applied potential,  $\gamma$ -PGA concentration positively correlated with charge output at 48 h

(Figure 2). The highest charge outputs of 36.49 ± 4.48 and 38.24 ± 2.46 Coulomb (C) were recorded at 400 and 600 mV, respectively, while the highest  $\gamma$ -PGA concentration was recorded at 400 mV (9.13 ± 1.4 g L<sup>-1</sup>). The optimal potential for subsequent EF experiments was therefore set at 400 mV. The low  $\gamma$ -PGA concentration at 600 mV can be attributed to a loss of membrane integrity of the cells, which might lead to seepage of intracellular reduced species, which, in turn, increase charge output (Krishnamurthi et al., 2020). The high potential could also lead to reduced cell viability, causing a decline in  $\gamma$ -PGA concentrations.

The high charge output of *B. subtilis* under oxidative potential indicates that this microorganism is a good platform for EF processes. The  $\gamma$ -PGA production recorded at 400 mV vs. Ag/AgCl (9.13 ± 1.25 g L<sup>-1</sup>) was higher than the value obtained at OCP (3.3 ± 0.99 g L<sup>-1</sup>). The difference between the maximum  $\gamma$ -PGA

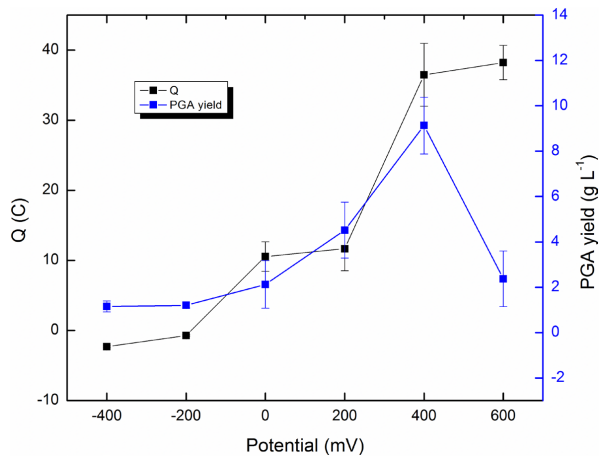


**FIGURE 2** Influence of applied potential on the total charge (Q) and  $\gamma$ -PGA production within the EPS of strain *B. subtilis* ATCC 6051. The optimal potential for EF experiments that leads to maximum  $\gamma$ -PGA concentration can be identified at 400 mV.

concentration recorded during the physiological experiments under F ( $6.39 \pm 0.94 \text{ g L}^{-1}$ ), and the value obtained in OCP experiments ( $3.3 \pm 0.99 \text{ g L}^{-1}$ ) is mainly due to the absence of agitation in the OCP experiments which was also the case with other EF experiments carried out. Facultatively anaerobic strains like *B. subtilis* can utilize oxygen as a terminal electron acceptor for the cells. Without agitation in conventional fermentation, oxygen dispersal within the medium is greatly reduced, thus reducing extracellular metabolite concentration. EF allows a circumvention of this challenge, as the electrode served as an electron acceptor with the aid of HNQ as redox mediator. With the use of a mediator compatible with the producing organism, the capacity of the electrode to function as an electron acceptor is increased as the cells do not necessary need direct individual contact with the electrode for extracellular electron transfer to occur. By virtue of this, both cells with and without direct contact to the electrode in the thin biofilm can be electrically controlled. In a similar study, Lai and colleagues cultivated the aerobic strain *Pseudomonas putida* under EF anoxic conditions, to convert glucose into organic acid with  $\text{K}_3[\text{Fe}(\text{CN})_6]$  as redox mediator. Despite the lack of dissolved oxygen, the bacteria thrived with an applied potential of 0.5V versus Ag/AgCl, showing a higher level of intracellular ATP and NADP<sup>+</sup>/NADPH than the OCP control experiment (Lai et al., 2016).

Other methods of enhancing biopolymer concentration have been attempted. A good example is the application of nutrient stress under F, when nitrogen-deficient medium was used to induce increased production of poly(3-hydroxybutyrate) (PHB) to up to approx.  $0.27 \text{ g L}^{-1}$  by *Ralstonia eutropha* (Miyahara et al., 2020). It was proposed that nutrient stress functioned by suppressing nucleic acid and protein synthesis in the bacteria causing a redirection of central carbon flux to the

synthesis of PHB. Despite the increased concentrations induced by nutrient stress, it is also worthy of note that EF had even previously been determined to enhance PHB production higher than F (OCP conditions) with up to  $1 \text{ g L}^{-1}$  in PHB, when EF was applied on *R. eutropha* (Nishio et al., 2013). This value represents over 350% increase in PHB produced by EF when compared with F. EF confers an advantage over F as it overcomes the limitations of cellular regulation by redox balance conferred on cells during F. The presence of an electrode in the fermentation system can cause an induced shift from redox balance to imbalance in fermentation, leading to an extended conversion of more substrates into products (Moscoviz et al., 2016). This process provides an additional respiratory pathway for the bacteria and an avenue to exceed the theoretical maxima usually obtained in F. This occurs as electric currents trigger the cells to increase metabolic rates by affecting the intracellular oxidation-reduction potential (ORP).

To further examine the value of EF in enhancing  $\gamma$ -PGA concentration in our work and confirm the presence of  $\gamma$ -PGA in *B. subtilis* EPS, we utilized a GM  $\gamma$ -PGA over-producing strain, *B. subtilis* PB5760, which exhibits  $\gamma$ -PGA biosynthesis exclusively in the presence of IPTG. Besides representing a non- $\gamma$ -PGA producer control strain when grown in the absence of IPTG, this strain was tested under the optimized EF conditions set for the WT strain (Figure 3 and Table S1). In F in the presence of IPTG, PB5760 produced up to  $15.42 \pm 1.45 \text{ g L}^{-1}$   $\gamma$ -PGA, which is about a 4.5-fold increase compared with  $3.44 \pm 1.55 \text{ g L}^{-1}$  generated by *B. subtilis* ATCC 6051 under OCP conditions. Using EF, we further improved the concentration to  $23.12 \pm 1.64 \text{ g L}^{-1}$ . The yield and productivity values of the concentrations of  $\gamma$ -PGA produced by the different *B. subtilis* strains under F and EF conditions are shown in Table S3. Highest yield in percentages showing grams of sugars converted to grams of  $\gamma$ -PGA reached 51.3% when genetically modified *B. subtilis* was used under EF conditions. This clearly showed the potential of EF bioprocesses to enhance  $\gamma$ -PGA concentrations in EPS. We demonstrated here that EF could be complementary to standard genetic modification of strains in boosting  $\gamma$ -PGA concentration. Without induction, the modified strain had near zero production of  $\gamma$ -PGA. As expected, there was no significant difference in the quantities of  $\gamma$ -PGA produced by WT strain with or without IPTG under both F and EF modes. These results demonstrated that IPTG had no influence on the overall concentration of  $\gamma$ -PGA except for functioning as an inducer for gene expression of the  $\gamma$ -PGA biosynthetic operon in the GM strain.

In electrofermentation, the use of polarized electrodes as terminal electron acceptors allows the process to be carried out under low/minimal aeration condition without significantly affecting  $\gamma$ -PGA yield. This is expected to reduce the cost of air supply and

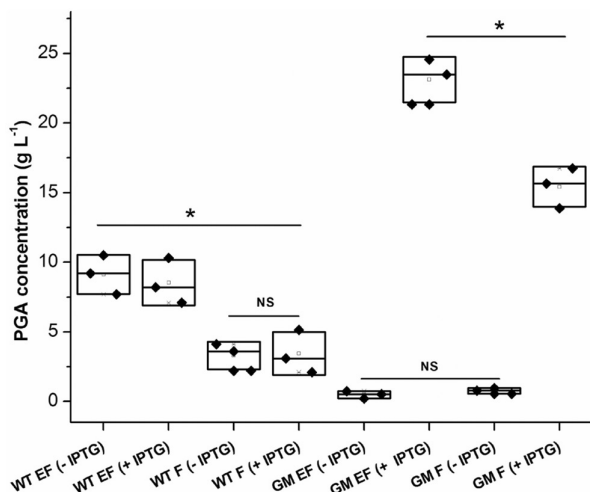


**FIGURE 3** Comparison of  $\gamma$ -PGA recovered within the EPS of *B. subtilis* ATCC 6051 (WT) and *B. subtilis* PB5760 (GM) under EF and F conditions with and without IPTG. F was carried out under OCP conditions, while EF was carried out at 0.4 V versus Ag/AgCl using a 9.6 cm<sup>2</sup> electrode surface area. Tukey test, \* $p < 0.05$ , NS, not significant.

stirring significantly. Further, electrofermentation allows fine-tuning of the terminal electron acceptor potential, which in turn enables optimizing the bioconversion process. While the actual cost benefits must be validated in a scale-up implementation of electrofermentation (currently ongoing in our group), and the cost of the electrical current sources must be factored in, there is reason to believe that electrofermentation coupled with biofilm can reduce the cost and improve the precision of current fermentation processes.

The addition of HNQ to the medium increases both the charge output and the  $\gamma$ -PGA (Figure S1). These data further confirmed that the increase in  $\gamma$ -PGA concentration under EF is due to the extracellular electron transfer to the polarized electrode, which is further enhanced in presence of a suitable redox mediator. EF has been identified as a practical means to improve the biotechnological applications of weak electroactive bacteria (Moscoviz et al., 2016). *Bacillus* sp., as weak electricigen, have been reported to produce flavins that act as natural mediators in electroactivity (Doyle & Marsili, 2018), but can also utilize externally added mediators in EF.

The enhancement of electroactivity in EF by addition of mediators has been adopted in biopolymer production by *Ralstonia eutropha* using poly(2-methacryloyloxyethyl phosphorylcholine co-vinylferrocene) (PMF) as a biocompatible mediator with a 60% increase of polyhydroxybutyrate (PHB) production (Nishio et al., 2013). Similarly, HNQ was utilized as a biocompatible mediator in the EF production of 3-hydroxypropionic acid (3-HP) from glycerol in a bioengineered *K. pneumoniae* strain overexpressing aldehyde dehydrogenase, leading to a 1.7-fold increase

in 3-HP yield (Kim et al., 2017). Based on the results reported and on previous studies, the proposed mechanism is illustrated in Figure 4. The exogenous mediator HNQ functions in combination with an electrode set at a sufficiently high oxidizing potential. With the assimilation of sugars and nitrogen sources by the cells during nutrition, the glycolytic pathway and tricarboxylic acid cycles are employed accordingly leading to the generation of electrons. The rate of electron generation and intracellular mobility of these electrons are facilitated by the activities of redox carriers such as NAD<sup>+</sup>/NADH which ultimately interact with membrane diffusible redox mediators such as the exogenously added HNQ. The electrode potential drives regulated electron flow from the cell based on the positive potential in the extracellular environment. Excess electrons generated can be stored as biopolymers as earlier explained (ter Heijne et al., 2021). Here, the extracellular accumulation of  $\gamma$ -PGA is observed as a direct effect of the electrode potential.

The FTIR spectra of  $\gamma$ -PGA enriched EPS samples (Figure 5) showed that the polymers produced under all conditions were similar in chemical composition, possessing similar functional groups in the range of 4000–500 cm<sup>-1</sup>. The spectral absorption (percentage transmittance) intensities, however, were slightly different for specific functional groups depending on the applied potential. There was a prominent peak between 3270 and 3300 cm<sup>-1</sup> in all samples, which is likely the strong absorption of O-H symmetric stretching vibration characteristic of an acid. The absorption peaks between 1650 and 1616 cm<sup>-1</sup> correspond to the –CONHR, asymmetric stretching vibration band, and C=O stretching characteristic of amides. The peak at around 1039 cm<sup>-1</sup> was attributed to the stretching vibration of C–N groups. Further peaks between 1000 and 500 cm<sup>-1</sup> are characteristic of in-plane bending and rocking vibrations attributed to (CH<sub>2</sub>) components ( $n > 4$ ) of  $\gamma$ -PGA. All peaks observed were in agreement with earlier reports of FT-IR spectra of  $\gamma$ -PGA (Mohanraj et al., 2019; Xavier et al., 2020). The differences in intensities of transmission of the different functional groups could be related to slight variations in the molecular weights of the polymer produced under different conditions. There were subtle differences in transmission intensities for the  $\gamma$ -PGA produced by the modified strain compared with the wild type, likely due to different molecular weight of  $\gamma$ -PGA in the two strains. Amino acid by-products could also be present in the extraction mix and justify the differences in chain lengths observed.

The (<sup>1</sup>H)-NMR spectra were obtained for  $\gamma$ -PGA-enriched EPS selected samples (Figure 6). The (<sup>1</sup>H)-NMR data confirmed the presence of the  $\alpha$  (3.5–4.2 ppm),  $\beta$  (2.01–1.75 ppm) and  $\gamma$  (2.1–2.3 ppm) regions typically associated with  $\gamma$ -PGA in samples derived from both the WT (Figure 6A) and GM strains

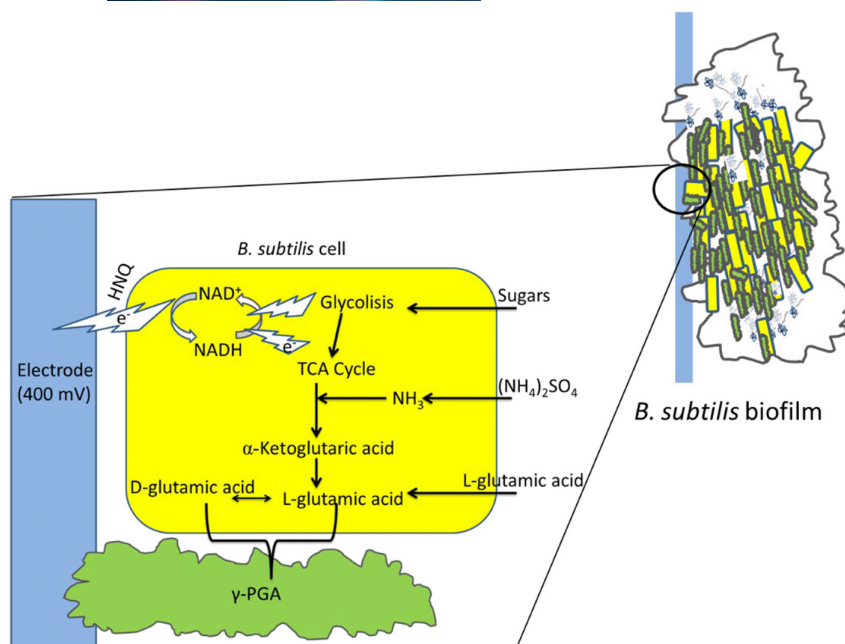


**FIGURE 4** Proposed mechanism of  $\gamma$ -PGA-enriched EPS production in *B. subtilis* biofilm under EF conditions. Electrical charges flow from cell to electrode increases electron cycling by the redox pair  $\text{NAD}^+/\text{NADH}$ , which regenerate electrons that are coupled with the main metabolic pathways for enhanced metabolic activities, subsequently increasing  $\gamma$ -PGA production and extracellular accumulation.

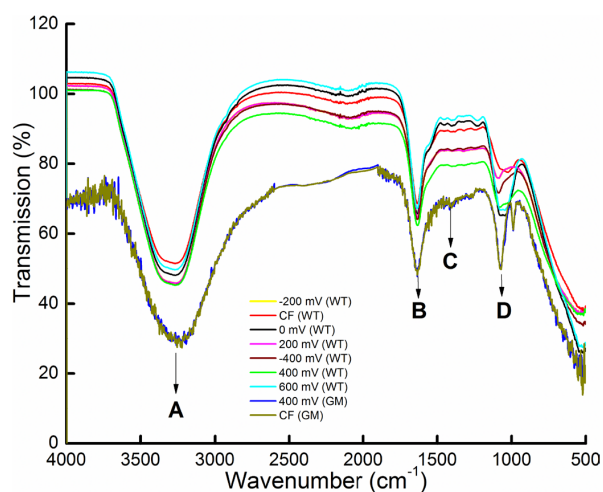


**FIGURE 5** Combined FT-IR spectra of  $\gamma$ -PGA-enriched EPS produced under F and EF at different potentials in WT and GM *B. subtilis* strains. (A) 3350–3450  $\text{cm}^{-1}$ , (B) 1659  $\text{cm}^{-1}$ , (C) 1500–1250  $\text{cm}^{-1}$ , (D) 1100  $\text{cm}^{-1}$ .

(Figure 6B,C). Some spectra showed the presence of amino acid residues from the EPS extracts, which are likely due to the close interactions between proteins and  $\gamma$ -PGA in biofilms; hence, other amides and amino acid residues formed during the fermentation process were detected. However, the majority of the samples analysed were consistent with the chemical structure of  $\gamma$ -PGA. To confirm the presence and chemical signature of  $\gamma$ -PGA in the EPS samples from the WT and GM strains,  $^1\text{H}$ -NMR was carried out in the presence (Figure 6B) and absence of IPTG (Figure 6C). The GM in IPTG-deficient medium did not show the characteristic  $\gamma$ -PGA peaks present

in the other conditions. The peaks observed in this sample were likely derived from other amino acids produced within the EPS (Figure 7). In general, the majority of the samples tested had similar  $^1\text{H}$ -NMR patterns and confirmed that the EPS was enriched with  $\gamma$ -PGA.

From the  $^1\text{H}$ -NMR data,  $\gamma$ -PGA produced under EF was similar to  $\gamma$ -PGA produced in F as shown by further  $^1\text{H}$ -NMR data (Figure S3A–C). The  $^1\text{H}$ -NMR spectra obtained from the  $\gamma$ -PGA produced by the GM strain under both F and EF conditions were also similar. The  $^1\text{H}$ -NMR spectra obtained in this work were consistent with earlier reports of  $^1\text{H}$ -NMR from  $\gamma$ -PGA (Xavier et al., 2020), and with the  $^1\text{H}$ -NMR characteristics of a  $\gamma$ -PGA standard (Wang, Kim, et al., 2020).

While  $^1\text{H}$ -NMR analysis is the ideal technique to confirm the production of  $\gamma$ -PGA in the F and EF process, it requires high-end equipment, which is unsuitable for real-time quantification of  $\gamma$ -PGA during the fermentation process. Thus, EIS was employed for rapid analysis and quantification of  $\gamma$ -PGA at the end of the F and EF process for both WT and GM strains. Biopolymer accumulation in biofilms increases the biofilm capacitance, due to the low conductivity of bacterial polymers (ter Heijne et al., 2018). The  $\gamma$ -PGA-enriched EPS produced by the WT strain under F and EF conditions (400 mV) have effective capacitance ( $C_{\text{eff}}$ ) of  $50.9 \pm 6.4$  and  $86.8 \pm 8.0 \mu\text{F cm}^{-2}$ , respectively (Figures 7A and S2). The effect of the applied potential on  $C_{\text{eff}}$  is similar in both the WT and the GM strains (Figure 7B, Tables S2 and S4). The  $C_{\text{eff}}$  of  $\gamma$ -PGA-EPS sample from GM strain under EF conditions was the highest ( $272.8 \pm 44.7 \mu\text{F cm}^{-2}$ ), due to the accumulation of  $\gamma$ -PGA in these samples. EIS, however, does not allow to determine the molecular weight of

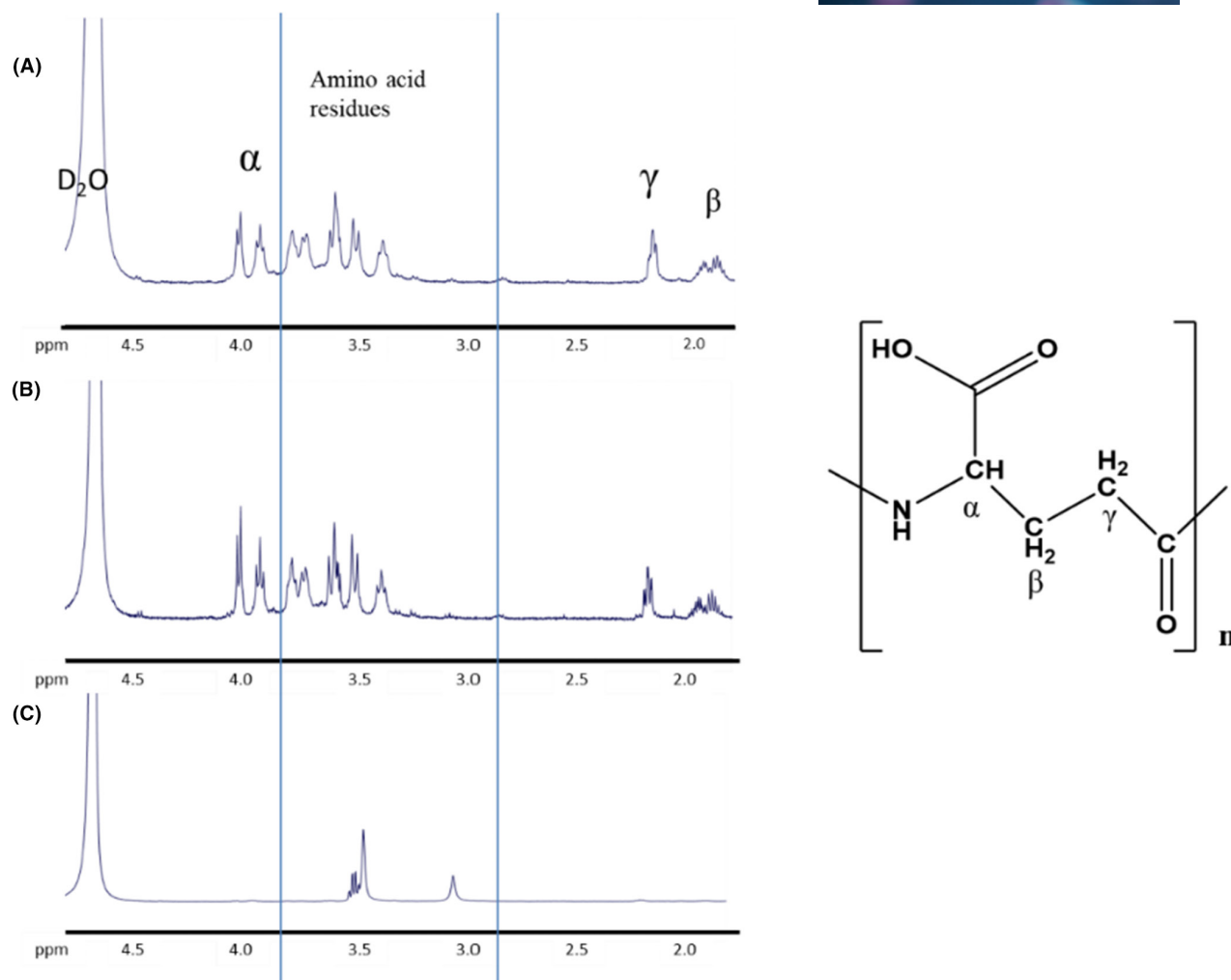


**FIGURE 6** Representative <sup>1</sup>H-NMR spectrum of  $\gamma$ -PGA-enriched EPS extracted from *B. subtilis* strains under EF conditions (A) WT (B) GM with IPTG induction. (C) GM without IPTG (negative control). Peaks corresponding to the  $\alpha$ : 4.1–3.9 ppm,  $\beta$ : 2.01–1.75 ppm;  $\gamma$ : 2.1–2.3 ppm regions of  $\gamma$ -PGA are identified in the samples positive for  $\gamma$ -PGA. Other peaks might be amino acid residues from the EPS after extraction. The GM grown in IPTG-deficient medium lacked the ability to produce  $\gamma$ -PGA, as confirmed by the absence of the  $\alpha$ ,  $\beta$  and  $\gamma$  regions peculiar to  $\gamma$ -PGA.

biopolymers or discriminate among different biopolymers that accumulate in the biofilm.

The presence of well-formed EPS indicates strong interactions between electrodes and cells under EF conditions. EF-conditioned cells of WT strain (Figure 8A) showed denser EPS structures when compared with control cultures grown without applied potentials (Figure 8B). Microscope analysis confirmed that EF conditions assisted the EPS-based  $\gamma$ -PGA formation. Similar observations were made for GM strain under EF and F, in which the EF conditions also showed higher cell densities than the F-grown cells (Figure S4).

The closely packed arrangement of the cells in the  $\gamma$ -PGA-enriched EPS indicated the presence of  $\gamma$ -PGA within the EPS in the biofilm. The images of the biofilms formed by the GM strain showed the presence of thick EPS structures, tightly bound to cells and electrodes (Figure S4). The microscopic structure of the

$\gamma$ -PGA-enriched EPS was also observed by SEM after extraction (Figure S5A–D), showing compact matter devoid of cells.

The EF conditions can alter metabolic fluxes, affecting the intracellular synthesis of  $\gamma$ -PGA. Within intracellular systems, the balance of redox activities is achieved by redox pairs like NAD<sup>+</sup>/NADH (Cai et al., 2017; Vassilev et al., 2021). The changes in extracellular and intracellular redox potentials induce the activities of key regulatory metabolic enzymes, which modulate electron flow using cycling mechanisms between redox pairs—NAD<sup>+</sup>/NADH (Tang et al., 2016). This redox pair has been identified as a major player in EF, especially when extracellular electron transfer (EET) is involved. In EET, the balance of electrons within the cell system is achieved by mopping up electrons or providing electrons through the electrode.

In a previous report by Choi et al. (2014) on butanol production from glucose under EF conditions, NADH

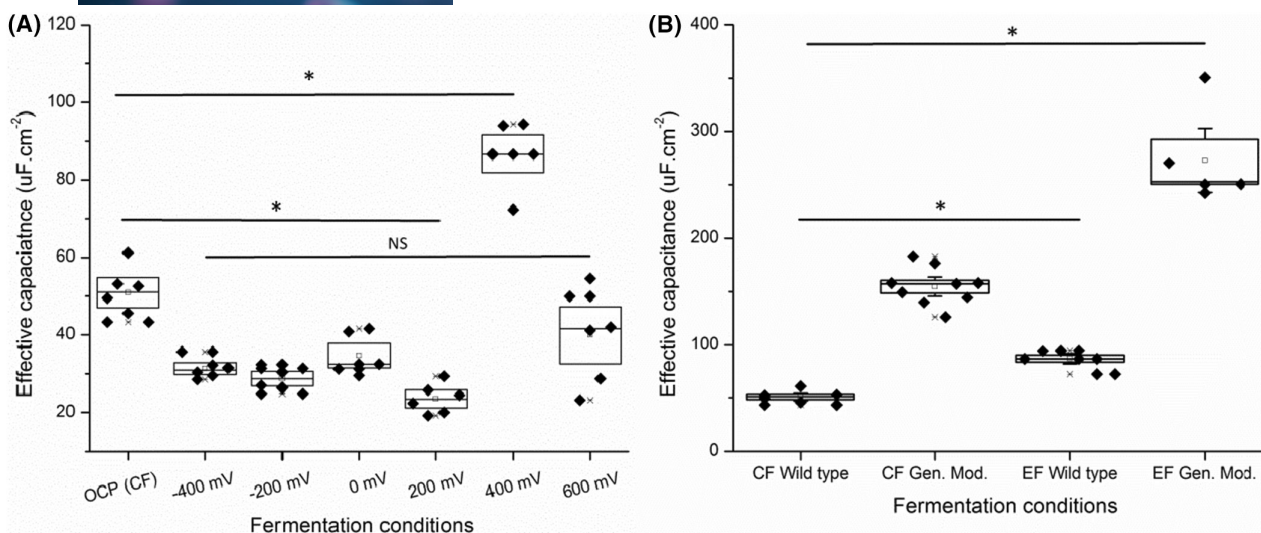


**FIGURE 7**  $C_{\text{eff}}$  of  $\gamma$ -PGA containing EPS samples from (A) EF and F of WT strain at optimum growth conditions, pH 7.4, and 35°C; (B) WT and GM strains under F and optimal potential (400 mV). All the modified strain experiments include addition of 0.3 mM IPTG. Tukey test, \* $p < 0.05$ , NS, not significant.

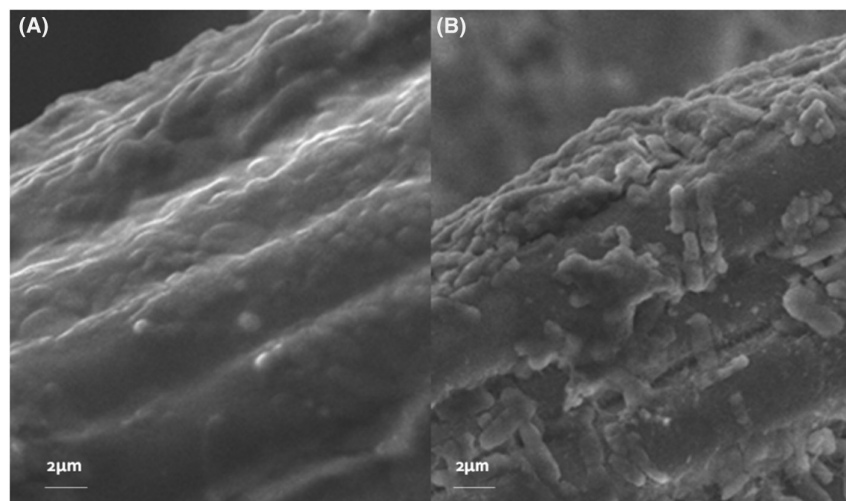


**FIGURE 8** SEM images of *B. subtilis* ATCC 6051 forming EPS containing  $\gamma$ -PGA on WE under (A) EF condition (400 mV), showing tightly packed cells on the electrode surface (B) OCP condition, showing loosely packed cells.

concentration was higher in EF. At increased NADH levels, the cells compensated producing more butanol and less hydrogen. The  $\text{NAD}^+/\text{NADH}$  ratio was eventually balanced similar to the ratio observed in the F; therefore, the goal of increasing butanol concentration was achieved through electrons supplied by EF to butanol synthesis. It has also been shown that exogenous redox mediators (e.g., HNQ) did not add any extra bioenergetic value to the rate of electronic modulation of substrate conversion to target metabolites (Moscoviz et al., 2016). Therefore, EF can be applied to numerous microbial species if a suitable redox mediator is employed.

We hypothesize that the effect of the applied potential observed in this work could drive glycolysis and TCA cycle upwards or downwards depending on the species-dependent carbon flux requirement. This electronic control of flux patterns for subsequent metabolic pathways downstream means that virtually any

metabolic pathway for any metabolite can be targeted in any bacteria as long as it is influenced by the breakdown of carbon substrates. The specificity of applied potentials has been evaluated in some earlier EF works. *Shewanella oneidensis* has previously been used in the production of ethanol at a poised potential of 203 mV versus Ag/AgCl by EF conversion of glycerol (Flynn et al., 2010). An engineered *E. coli* strain had also been induced at 0 mV versus Ag/AgCl to convert glycerol to ethanol and acetate under EF, using methylene blue as a mediator (Sturm-Richter et al., 2015). The specific EF potential depends on the use of either the cathode or anode as the working electrode (Moscoviz et al., 2016).

## CONCLUSIONS

The concentration of  $\gamma$ -PGA produced within the EPS of *B. subtilis* was improved by the optimization of

the carbon and nitrogen sources in the fermentation medium. Electrofermentation at 400 mV increased  $\gamma$ -PGA biosynthesis in both wild-type and  $\gamma$ -PGA over-producing *B. subtilis* strains. The specific presence of  $\gamma$ -PGA in the EPS was confirmed by ( $^1\text{H}$ )-NMR. SEM imaging showed exopolymer formations within biofilms under EF conditions for both the wild type and the  $\gamma$ -PGA over-producing *B. subtilis* strains. The positive impact of electrofermentation on  $\gamma$ -PGA concentration in *B. subtilis* could be linked to the intracellular concentration of  $\text{NAD}^+/\text{NADH}$ , which directly affect glycolysis and tricarboxylic acid cycle activities within the cell, generating the needed precursors and metabolites. Electrofermentation is a promising technique to improve the production of  $\gamma$ -PGA and other important bioproducts. Moreover, electrofermentation can be combined with biofilm intensification to increase concentration of biopolymers in conventional bioprocesses.

## AUTHOR CONTRIBUTIONS

**Alina Adilkhanova:** Data curation (equal); investigation (equal). **Anar Ormantayeva:** Investigation (supporting). **Aisholpan Kaziullayeva:** Investigation (supporting). **Kayode Olaifa:** Investigation (supporting); methodology (equal). **Neda Eghtesadi:** Investigation (supporting). **Azza H. Abbas:** Writing – review and editing (supporting). **Cinzia Calvio:** Methodology (equal); writing – review and editing (equal). **Tri Pham:** Supervision (supporting); writing – review and editing (supporting). **Obinna Ajunwa:** Conceptualization (equal); data curation (lead); methodology (equal); writing – original draft (lead); writing – review and editing (equal). **Enrico Marsili:** Conceptualization (lead); data curation (supporting); funding acquisition (lead); methodology (lead); supervision (lead); writing – original draft (supporting); writing – review and editing (lead).

## ACKNOWLEDGEMENTS

This work was supported by the Collaborative Research Program 021220CRP0522, Nazarbayev University, Kazakhstan. This work was partially supported by the Nottingham Ningbo China Beacons of Excellence Research and Innovation Institute (budget code I01220800007).

## CONFLICT OF INTEREST STATEMENT

The authors declare that they have no known competing interests of any kind.

## ORCID

Enrico Marsili  <https://orcid.org/0000-0003-3150-1564>

## REFERENCES

Arnold, A., Sajitz-Hermstein, M. & Nikoloski, Z. (2015) Effects of varying nitrogen sources on amino acid synthesis costs in

*Arabidopsis thaliana* under different light and carbon-source conditions. *PLoS ONE*, 10, 1–22. Available from: <https://doi.org/10.1371/journal.pone.0116536>

- Bajaj, I.B., Lele, S.S. & Singhal, R.S. (2009) A statistical approach to optimization of fermentative production of poly( $\gamma$ -glutamic acid) from *Bacillus licheniformis* NCIM 2324. *Bioresource Technology*, 100, 826–832. Available from: <https://doi.org/10.1016/j.biortech.2008.06.047>
- Biswas, M.C., Jony, B., Nandy, P.K., Chowdhury, R.A., Halder, S., Kumar, D. et al. (2022) Recent advancement of biopolymers and their potential biomedical applications. *Journal of Polymers and the Environment*, 30, 51–74. Available from: <https://doi.org/10.1007/s10924-021-02199-y>
- Cai, D., He, P., Lu, X., Zhu, C., Zhu, J., Zhan, Y. et al. (2017) A novel approach to improve poly- $\gamma$ -glutamic acid production by NADPH regeneration in *Bacillus licheniformis* WX-02. *Scientific Reports*, 7, 1–9. Available from: <https://doi.org/10.1038/srep43404>
- Choi, O., Kim, T., Woo, H.M. & Um, Y. (2014) Electricity-driven metabolic shift through direct electron uptake by electroactive heterotroph *Clostridium pasteurianum*. *Scientific Reports*, 4, 6961. Available from: <https://doi.org/10.1038/srep06961>
- Doyle, L.E. & Marsili, E. (2018) Weak electricigens: a new avenue for bioelectrochemical research. *Bioresource Technology*, 258, 354–364. Available from: <https://doi.org/10.1016/j.biortech.2018.02.073>
- Ermoli, F., Bontà, V., Vitali, G. & Calvio, C. (2021) SwrA as global modulator of the two-component system DegS in *Bacillus subtilis*. *Research in Microbiology*, 172, 103877. Available from: <https://doi.org/10.1016/j.resmic.2021.103877>
- Flemming, H.C., Wingender, J., Szewzyk, U., Steinberg, P., Rice, S.A. & Kjelleberg, S. (2016) Biofilms: an emergent form of bacterial life. *Nature Reviews Microbiology*, 14, 563–575. Available from: <https://doi.org/10.1038/nrmicro.2016.94>
- Flynn, J.M., Ross, D.E., Hunt, K.A., Bond, D.R. & Gralnick, J.A. (2010) Enabling unbalanced fermentations by using engineered electrode-interfaced bacteria. *MBio*, 1, 1–8. Available from: <https://doi.org/10.1128/mBio.00190-10>
- Förster, A.H. & Gescher, J. (2014) Metabolic engineering of *Escherichia coli* for production of mixed-acid fermentation end products. *Frontiers in Bioengineering and Biotechnology*, 2, 1–12. Available from: <https://doi.org/10.3389/fbioe.2014.00016>
- Gao, W., He, Y., Zhang, F., Zhao, F., Huang, C., Zhang, Y. et al. (2019) Metabolic engineering of *Bacillus amyloliquefaciens* LL3 for enhanced poly- $\gamma$ -glutamic acid synthesis. *Microbial Biotechnology*, 12, 932–945. Available from: <https://doi.org/10.1111/1751-7915.13446>
- Ju, W.T., Song, Y.S., Jung, W.J. & Park, R.D. (2014) Enhanced production of poly- $\gamma$ -glutamic acid by a newly-isolated *Bacillus subtilis*. *Biotechnology Letters*, 36, 2319–2324. Available from: <https://doi.org/10.1007/s10529-014-1613-3>
- Kim, C., Kim, M.Y., Michie, I., Jeon, B.H., Premier, G.C., Park, S. et al. (2017) Anodic electro-fermentation of 3-hydroxypropionic acid from glycerol by recombinant *Klebsiella pneumoniae* L17 in a bioelectrochemical system. *Biotechnology for Biofuels*, 10, 1–11. Available from: <https://doi.org/10.1186/s13068-017-0886-x>
- Konkol, M.A., Blair, K.M. & Kearns, D.B. (2013) Plasmid-encoded ComI inhibits competence in the ancestral 3610 strain of *Bacillus subtilis*. *Journal of Bacteriology*, 195, 4085–4093. Available from: <https://doi.org/10.1128/JB.00696-13>
- Krishnamurthi, V.R., Rogers, A., Peifer, J., Niyonshuti, I.I., Chen, J. & Wang, Y. (2020) Microampere electric current causes bacterial membrane damage and two-way leakage in a short period of time. *Applied and Environmental Microbiology*, 86, 1–10. Available from: <https://doi.org/10.1128/AEM.01015-20>
- Lai, B., Yu, S., Bernhardt, P.V., Rabaey, K., Virdis, B. & Krömer, J.O. (2016) Anoxic metabolism and biochemical production in

- Pseudomonas putida* F1 driven by a bioelectrochemical system. *Biotechnology for Biofuels*, 9, 1–13. Available from: <https://doi.org/10.1186/s13068-016-0452-y>
- Li, F., Li, Y.X., Cao, Y.X., Wang, L., Liu, C.G., Shi, L. et al. (2018) Modular engineering to increase intracellular NAD(H<sup>+</sup>) promotes rate of extracellular electron transfer of *Shewanella oneidensis*. *Nature Communications*, 9, 1–13. Available from: <https://doi.org/10.1038/s41467-018-05995-8>
- Li, S.W., Sheng, G.P., Cheng, Y.Y. & Yu, H.Q. (2016) Redox properties of extracellular polymeric substances (EPS) from electroactive bacteria. *Scientific Reports*, 6, 1–7. Available from: <https://doi.org/10.1038/srep39098>
- Liu, S., Li, P., Liu, X., Wang, P., Xue, W., Ren, Y. et al. (2021) Bioinspired mineral-polymeric hybrid hyaluronic acid/poly ( $\gamma$ -glutamic acid) hydrogels as tunable scaffolds for stem cells differentiation. *Carbohydrate Polymers*, 264, 118048. Available from: <https://doi.org/10.1016/j.carbpol.2021.118048>
- Logan, B.E., Rossi, R., Ragab, A. & Saikaly, P.E. (2019) Electroactive microorganisms in bioelectrochemical systems. *Nature Reviews Microbiology*, 17, 307–319. Available from: <https://doi.org/10.1038/s41579-019-0173-x>
- Luo, Z., Guo, Y., Liu, J., Qiu, H., Zhao, M., Zou, W. et al. (2016) Microbial synthesis of poly- $\gamma$ -glutamic acid: current progress, challenges, and future perspectives. *Biotechnology for Biofuels*, 9, 1–12. Available from: <https://doi.org/10.1186/s13068-016-0537-7>
- Miyahara, Y., Yamamoto, M., Thorbecke, R., Mizuno, S. & Tsuge, T. (2020) Autotrophic biosynthesis of polyhydroxyalkanoate by *Ralstonia eutropha* from non-combustible gas mixture with low hydrogen content. *Biotechnology Letters*, 42, 1655–1662. Available from: <https://doi.org/10.1007/s10529-020-02876-3>
- Mohanraj, R., Gnanamangai, B.M., Ramesh, K., Priya, P., Srisunmathi, R., Poornima, S. et al. (2019) Optimized production of gamma poly glutamic acid ( $\gamma$ -PGA) using sago. *Biocatalysis and Agricultural Biotechnology*, 22, 101413. Available from: <https://doi.org/10.1016/j.bcab.2019.101413>
- Moscoviz, R., Toledo-Alarcón, J., Trably, E. & Bernet, N. (2016) Electro-fermentation: how to drive fermentation using electrochemical systems. *Trends in Biotechnology*, 34, 856–865. Available from: <https://doi.org/10.1016/j.tibtech.2016.04.009>
- Nair, P., Navale, G.R. & Dharne, M.S. (2021) Poly-gamma-glutamic acid biopolymer: a sleeping giant with diverse applications and unique opportunities for commercialization. *Biomass Conversion and Biorefinery*, 13, 4555–4573. Available from: <https://doi.org/10.1007/s13399-021-01467-0>
- Nishio, K., Kimoto, Y., Song, J., Konno, T., Ishihara, K., Kato, S. et al. (2013) Extracellular electron transfer enhances polyhydroxybutyrate productivity in *Ralstonia eutropha*. *Environmental Science and Technology Letters*, 1, 40–43. Available from: <https://doi.org/10.1021/ez400085b>
- Odeniyi, O. & Avoseh, D. (2018) Effects of media components and agricultural by-products on  $\gamma$ -polyglutamic acid production by *Bacillus toyonensis* As8. *Polymers in Medicine*, 48, 91–97. Available from: <https://doi.org/10.17219/pim/105555>
- Qiu, Y., Wang, Q., Zhu, C., Yang, Q., Zhou, S., Xiang, Z. et al. (2019) Deciphering metabolic responses of biosurfactant lichenysin on biosynthesis of poly- $\gamma$ -glutamic acid. *Applied Microbiology and Biotechnology*, 103, 4003–4015. Available from: <https://doi.org/10.1007/s00253-019-09750-x>
- Richard, A. & Margaritis, A. (2003) Optimization of cell growth and poly(glutamic acid) production in batch fermentation by *Bacillus subtilis*. *Biotechnology Letters*, 25, 465–468. Available from: <https://doi.org/10.1023/A:1022644417429>
- Sanda, F., Fujiyama, T. & Endo, T. (2001) Chemical synthesis of poly- $\gamma$ -glutamic acid by polycondensation of  $\gamma$ -glutamic acid dimer: synthesis and reaction of poly- $\gamma$ -glutamic acid methyl ester. *Journal of Polymer Science, Part A: Polymer Chemistry*, 39, 732–741. Available from: [https://doi.org/10.1002/1099-0518\(20010301\)39:5<732::AID-POLA1045>3.0.CO;2-P](https://doi.org/10.1002/1099-0518(20010301)39:5<732::AID-POLA1045>3.0.CO;2-P)
- Scoffone, V., Dondi, D., Biino, G., Borghese, G., Pasini, D., Galizzi, A. et al. (2013) Knockout of *pgdS* and *ggt* genes improves  $\gamma$ -PGA yield in *B. subtilis*. *Biotechnology and Bioengineering*, 110, 2006–2012. Available from: <https://doi.org/10.1002/bit.24846>
- Song, Y., Zhang, Y., He, M., Liu, H., Hu, C., Yang, L. et al. (2020) Enhancing the production of poly- $\gamma$ -glutamate in *Bacillus subtilis* ZJS18 by the heat- and osmotic shock and its mechanism. *Preparative Biochemistry and Biotechnology*, 50, 1023–1030. Available from: <https://doi.org/10.1080/10826068.2020.1780610>
- Sturm-Richter, K., Golitsch, F., Sturm, G., Kipf, E., Dittrich, A., Beblawy, S. et al. (2015) Unbalanced fermentation of glycerol in *Escherichia coli* via heterologous production of an electron transport chain and electrode interaction in microbial electrochemical cells. *Bioresource Technology*, 186, 89–96. Available from: <https://doi.org/10.1016/j.biortech.2015.02.116>
- Tang, B., Zhang, D., Li, S., Xu, Z., Feng, X. & Xu, H. (2016) Enhanced poly( $\gamma$ -glutamic acid) production by H<sub>2</sub>O<sub>2</sub>-induced reactive oxygen species in the fermentation of *Bacillus subtilis* NX-2. *Biotechnology and Applied Biochemistry*, 63, 625–632. Available from: <https://doi.org/10.1002/bab.1416>
- ter Heijne, A., Liu, D., Sulonen, M., Sleutels, T. & Fabregat-Santiago, F. (2018) Quantification of bio-anode capacitance in bioelectrochemical systems using electrochemical impedance spectroscopy. *Journal of Power Sources*, 400, 533–538. Available from: <https://doi.org/10.1016/j.jpowsour.2018.08.003>
- ter Heijne, A., Pereira, M.A., Pereira, J. & Sleutels, T. (2021) Electron storage in electroactive biofilms. *Trends in Biotechnology*, 39, 34–42. Available from: <https://doi.org/10.1016/j.tibtech.2020.06.006>
- Vassilev, I., Aversch, N.J.H., Ledezma, P. & Kokko, M. (2021) Anodic electro-fermentation: empowering anaerobic production processes via anodic respiration. *Biotechnology Advances*, 48, 107728. Available from: <https://doi.org/10.1016/j.biotechadv.2021.107728>
- Wang, C., Wang, B., Zou, S., Wang, B., Liu, G., Zhang, F. et al. (2021) Cyclo- $\gamma$ -polyglutamic acid-coated dual-responsive nanomicelles loaded with doxorubicin for synergistic chemophotodynamic therapy. *Biomaterials Science*, 9, 5977–5987. Available from: <https://doi.org/10.1039/d1bm00713k>
- Wang, D., Hwang, J.S., Kim, D.H., Lee, S., Kim, D.H. & Joe, M.H. (2020a) A newly isolated *Bacillus siamensis* SB1001 for mass production of poly- $\gamma$ -glutamic acid. *Process Biochemistry*, 92, 164–173. Available from: <https://doi.org/10.1016/j.procbio.2019.11.034>
- Wang, D., Kim, H., Lee, S., Kim, D.H. & Joe, M.H. (2020b) Simultaneous production of poly- $\gamma$ -glutamic acid and 2,3-butanediol by a newly isolated *Bacillus subtilis* CS13. *Applied Microbiology and Biotechnology*, 104, 7005–7021. Available from: <https://doi.org/10.1007/s00253-020-10755-0>
- Westlake, J.R., Tran, M.W., Jiang, Y., Zhang, X., Burrows, A.D. & Xie, M. (2023) Biodegradable biopolymers for active packaging: demand, development and directions. *Sustainable Food Technology*, 1, 50–72. Available from: <https://doi.org/10.1039/D2FB00004K>
- Weusthuis, R.A., Lamot, I., van der Oost, J. & Sanders, J.P.M. (2011) Microbial production of bulk chemicals: development of anaerobic processes. *Trends in Biotechnology*, 29, 153–158. Available from: <https://doi.org/10.1016/j.tibtech.2010.12.007>
- Xavier, J.R., Madhan Kumarr, M.M., Natarajan, G., Ramana, K.V. & Semwal, A.D. (2020) Optimized production of poly ( $\gamma$ -glutamic acid) ( $\gamma$ -PGA) using *Bacillus licheniformis* and its application as cryoprotectant for probiotics. *Biotechnology and Applied Biochemistry*, 67, 892–902. Available from: <https://doi.org/10.1002/bab.1879>

- Xia, S., Zhang, L., Davletshin, A., Li, Z., You, J. & Tan, S. (2020) Application of polysaccharide biopolymer in petroleum recovery. *Polymers*, 12, 1–36. Available from: <https://doi.org/10.3390/POLYM12091860>
- Yu, Y., Yan, F., Chen, Y., Jin, C., Guo, J.H. & Chai, Y. (2016) Poly- $\gamma$ -glutamic acids contribute to biofilm formation and plant root colonization in selected environmental isolates of *Bacillus subtilis*. *Frontiers in Microbiology*, 7, 1–15. Available from: <https://doi.org/10.3389/fmicb.2016.01811>
- Yu, Y.Y., Zhai, D.D., Si, R.W., Sun, J.Z., Liu, X. & Yong, Y.C. (2017) Three-dimensional electrodes for high-performance bioelectrochemical systems. *International Journal of Molecular Sciences*, 18, 90. Available from: <https://doi.org/10.3390/ijms18010090>
- Zeng, W., Chen, G., Wang, Q., Zheng, S., Shu, L. & Liang, Z. (2014) Metabolic studies of temperature control strategy on poly( $\gamma$ -glutamic acid) production in a thermophilic strain *Bacillus subtilis* GXA-28. *Bioresource Technology*, 155, 104–110. Available from: <https://doi.org/10.1016/j.biortech.2013.12.086>
- Zeng, W., Chen, G., Zhang, Y., Wu, K. & Liang, Z. (2012) Studies on the UV spectrum of poly( $\gamma$ -glutamic acid) based on development of a simple quantitative method. *International Journal of Biological Macromolecules*, 51, 83–90. Available from: <https://doi.org/10.1016/j.ijbiomac.2012.04.005>
- Zhu, L., Chen, J., Mao, X. & Tang, S. (2021) A  $\gamma$ -PGA/KGM-based injectable hydrogel as immunoactive and antibacterial wound dressing for skin wound repair. *Materials Science and Engineering C*, 129, 112374. Available from: <https://doi.org/10.1016/j.msec.2021.112374>

## SUPPORTING INFORMATION

Additional supporting information can be found online in the Supporting Information section at the end of this article.

**How to cite this article:** Adilkhanova, A., Ormantayeva, A., Kaziullayeva, A., Olaifa, K., Egtesadi, N., Abbas, A.H. et al. (2024) Electrofermentation increases concentration of poly  $\gamma$ -glutamic acid in *Bacillus subtilis* biofilms. *Microbial Biotechnology*, 17, e14426. Available from: <https://doi.org/10.1111/1751-7915.14426>